

Lifting Line Theory for Supersonic Flow Applications

I. Jadic*

Institute of Applied Mathematics, Bucharest, Romania

and

V. N. Constantinescu†

Polytechnical Institute, Bucharest, Romania

The paper is devoted to the study of a supersonic lifting line theory intended to provide both a means of aerodynamic calculation and a benchmark for the validation of the control point position for the related constant pressure panel methods. The model is based on the small perturbations assumption. A constant distribution of bound vortices is assumed along the chord whereas the spanwise load distribution is calculated by means of trigonometrical series, formally similar to the subsonic methods. The calculated aerodynamic coefficients are in good agreement with the reference data, the precision being compatible with the small perturbations assumption. The control point position obtained is shown to vary as a function of aspect ratio from 100 to 88% of the local chord.

I. Introduction

LIFTING line theories might be regarded as one of the earliest computational fluid dynamics attempts. For example, Prandtl's simple lifting line theory¹ provided such a straightforward approach that the necessary calculations could be performed manually. Actually, most of the lifting line theories preceded the electronic computing equipment era, and as such were devised keeping in mind the calculation capabilities available until the middle of our century.

The explosive development of modern computers and computing techniques led a revolution within the computational fluid dynamics field. The more powerful the computers, the more complicated the problems tackled. Today the lifting line theories are no longer in current use since one can resort to a panel method within an affordable computational effort. However, it should be recognized that they brought valuable insight that helped the development of panel methods.

The aim of the present paper is to define a lifting line theory for supersonic flows within the small perturbations assumptions. Even if the interest of such an aerodynamical calculation method is limited, it is possible to use this approach to clarify some aspects concerning constant pressure panel methods (CPM) of the Woodward type,^{2,3} especially the control point positioning.

Supersonic lifting line theory (SLLT) is based primarily on the linearized potential equation for supersonic flow

$$(M_\infty^2 - 1) \frac{\partial^2 \varphi}{\partial x^2} - \frac{\partial^2 \varphi}{\partial y^2} - \frac{\partial^2 \varphi}{\partial z^2} = 0 \quad (1)$$

The second assumption that was made in the derivation of SLLT⁴ concerns the chordwise load distribution that was chosen to be constant

$$\gamma(x, y) = \gamma(y) \quad (2)$$

This constant chordwise load distribution ensures agreement with Ackeret's two-dimensional theory⁵ in the limiting case of infinite aspect ratio wings with supersonic edges. In

addition, the approximation (2) makes it possible to consider SLLT as a discretization with one panel chordwise for CPM.

Several works related to the present approach may be cited. To calculate the downwash behind wings in supersonic flows, Mirels and Haefeli⁶ have used a supersonic lifting line model whereas Laschka⁷ has used a constant chord loading model. However, in both approaches the wing loading had to be predetermined by means of other methods.

II. Calculation of Induced Velocities

A. General

In Ref. 8 a formula was derived for the calculation of the velocity induced by a vortex distribution within the small perturbations approximation. Thus, the continuity equation can be written

$$(M_\infty^2 - 1) \frac{\partial u}{\partial x} - \frac{\partial v}{\partial y} - \frac{\partial w}{\partial z} = 0 \quad (1a)$$

where the induced velocity \bar{V} is

$$\bar{V} = u\bar{i} + v\bar{j} + w\bar{k} \quad (3)$$

and corresponds to a known distribution of vortices $\bar{\Omega} = \text{curl } \bar{V}$ extending over a certain region D .

In the process of deriving the formula relating the induced velocity \bar{V} to the distribution of vortices $\bar{\Omega}$, the following "hyperbolic" operators, similar to Hamilton's "nabla" ones, are used:

$$\text{gradh } Y = \nabla^H Y = (M_\infty^2 - 1) \frac{\partial Y}{\partial x} \bar{i} - \frac{\partial Y}{\partial y} \bar{j} - \frac{\partial Y}{\partial z} \bar{k} \quad (4a)$$

$$\text{divh } \bar{X} = (\nabla^H \cdot \bar{X}) = (M_\infty^2 - 1) \frac{\partial X_1}{\partial x} - \frac{\partial X_2}{\partial y} - \frac{\partial X_3}{\partial z} \quad (4b)$$

$$\Delta^H Y = (M_\infty^2 - 1) \frac{\partial^2 Y}{\partial x^2} - \frac{\partial^2 Y}{\partial y^2} - \frac{\partial^2 Y}{\partial z^2} \quad (4c)$$

$$\begin{aligned} \text{curlh } \bar{X} = \nabla^H \times \bar{X} = & \left(-\frac{\partial X_3}{\partial y} + \frac{\partial X_2}{\partial z} \right) \bar{i} \\ & - \left[(M_\infty^2 - 1) \frac{\partial X_3}{\partial x} + \frac{\partial X_1}{\partial z} \right] \bar{j} + \left[(M_\infty^2 - 1) \frac{\partial X_2}{\partial x} + \frac{\partial X_1}{\partial y} \right] \bar{k} \end{aligned} \quad (4d)$$

Presented as Paper 91-5058 at the AIAA 3rd International Aerospace Planes Conference, Orlando, FL, Dec. 3-5, 1991; received Feb. 11, 1992; revision received Aug. 3, 1992; accepted for publication Aug. 12, 1992. Copyright © 1992 by the American Institute of Aeronautics and Astronautics, Inc. All rights reserved.

*Head, Department of Numerical Simulation in Fluid Mechanics, Bd. Păcii 220, Sect. 6.

†Professor, Aeronautical Engineering Faculty.

It must be noted that the similitude between the defined "hyperbolic" operators (4) and nabla ones is a purely formal one. For example,

$$\operatorname{divh} \operatorname{gradh} Y \neq \Delta^H Y$$

but

$$\operatorname{divh} \operatorname{grad} Y = \Delta^H Y$$

Let us designate by $M(x_M, y_M, z_M)$ the point where the induced velocity is calculated and by $P(x_P, y_P, z_P)$ a point in the domain D . Then the problem may be stated⁸ as

$$\operatorname{divh} \bar{V} = 0 \quad (5)$$

$$\begin{aligned} \operatorname{curl} \bar{V} &= \bar{\Omega} & \text{on } D \\ &= 0 & \text{on } D_1 = R^3 \setminus D \end{aligned} \quad (6)$$

In addition, if Σ is the surface bordering on D

$$\bar{n} \cdot \bar{\Omega}|_{\Sigma} = 0 \quad (7)$$

whereas $\operatorname{div} \bar{\Omega} = 0$ since $\operatorname{div} \operatorname{curl} \bar{V} = 0$.

The solution of this problem is the equivalent of the Biot-Savart formula for supersonic flow⁸

$$\bar{V}(M) = -\frac{1}{2\pi} \operatorname{curlh} \int_{D'(M)} \frac{\bar{\Omega}(P)}{r^H} d\tau_P \quad (8)$$

where $D'(M)$ is that part of D lying in the interior of the upstream Mach cone with apex in M , and

$$r^H = \sqrt{(x_M - x_P)^2 - (M_\infty^2 - 1)[(y_M - y_P)^2 + (z_M - z_P)^2]} \quad (9)$$

It is important to note here that the solution (8) allows us to calculate the vortex-induced velocities without making use of the so-called "finite part" of the integral (for a discussion of the finite part concept see Ref. 9), a mathematical notion difficult to relate to a physical meaning.

In the following it will be assumed that $M_\infty = \sqrt{2}$. Any other case can be treated this way by means of a Prandtl-Glauert transformation.

B. Supersonic Lifting Line Theory Equation

To derive the formula relating the induced velocity in point M and the vortex distribution on the wing in the SLLT approximation, the strip hypothesis is used.^{4,10} Moreover, it is assumed that the singularity occurring because of the free vortices in the proximity of the control point (when $y_P = y_M$) is to be treated according to Cauchy's principal part.

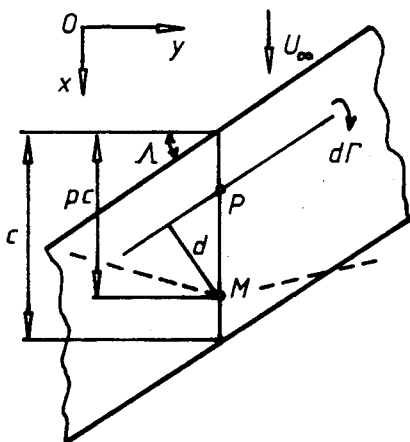


Fig. 1 Sweep angle.

The vortex horseshoe system on the wing has its bound part parallel to the Oy axis (see Fig. 1) whereas its free filaments are parallel to the freestream velocity (along Ox).

It can be shown that under these assumptions, the formula for the induced velocity takes the form^{4,10}

$$\begin{aligned} w(M) = & -\frac{1}{2\pi} \lim_{\epsilon \rightarrow 0} \left\{ \frac{2\gamma}{\epsilon} [x_M - x_{LE}(y_M)] \right. \\ & - \int_{-b/2}^{y_M - \epsilon} G(x_M, y_M, y_P) dy_P \\ & \left. - \int_{y_M + \epsilon}^{b/2} G(x_M, y_M, y_P) dy_P \right\} \end{aligned} \quad (10)$$

where LE is the leading edge, TE the trailing edge, and

$$r_{LE}^H(y_P) = \sqrt{[x_M - x_{LE}(y_P)]^2 - (y_M - y_P)^2 - z_M^2} \quad (11)$$

$$G(x_M, y_M, y_P) = \frac{\gamma(y_P)}{(y_P - y_M)^2} [r_{LE}^H(y_P) - r_S^H(y_P)] \quad (12)$$

$$\begin{aligned} [r_S^H(y_P)]^2 &= F \equiv [x_{TE}(y_P) - x_M]^2 - (y_P - y_M)^2 & \text{for } F > 0 \\ &= 0 & \text{otherwise} \end{aligned} \quad (13)$$

whereas b is the span of the wing (the plane $y = 0$ is assumed to be located at the midspan of wing).

Finally, the integral equation that will yield the spanwise loading is obtained by means of the kinematic condition

$$w = -U_\infty \alpha(y) \quad (14)$$

where $\alpha(y)$ is the local incidence, and w is given by Eq. (10).

III. Position of the Control Point

As already mentioned, assumption (2) ensures that SLLT will agree with Ackeret's two-dimensional flat plate theory⁵ when the aspect ratio tends to infinity and the edges are supersonic. Since this is true for any control point position,¹¹ we shall examine the limiting cases of very small aspect ratios and very large aspect ratios with subsonic edges.

A. Very Small Aspect Ratio Wings

Jones's small aspect ratio wing theory¹² shows that the aerodynamic characteristics are unaltered by the Mach number. For a quasidelta ("pointed") wing with constant slope (flat plate), the spanwise distribution of circulation is elliptical

$$\Gamma = \Gamma_0 \sqrt{1 - \frac{y^2}{(b/2)^2}} \quad (15)$$

The slope of the lift coefficient with respect to the angle of incidence α is

$$C_{L_\alpha} = \frac{\pi}{2} A, \quad A = b^2/S \quad (16)$$

where A is the aspect ratio and S the area of the wing.

Moreover, we shall assume that the trailing edge of the wing under consideration is supersonic, i.e., $r_S^H = 0$.

Thus, Eqs. (10) and (14) yield

$$\begin{aligned} U_\infty \alpha = & \frac{p}{2\pi} \lim_{\epsilon \rightarrow 0} \left[\frac{2\Gamma(y_M)}{\epsilon} - \int_{-b/2}^{y_M - \epsilon} \frac{\Gamma(y_P)}{(y_P - y_M)^2} dy_P \right. \\ & \left. - \int_{y_M + \epsilon}^{b/2} \frac{\Gamma(y_P)}{(y_P - y_M)^2} dy_P \right] \end{aligned} \quad (17)$$

where

$$p = \frac{x_M - x_{LE}(y_P)}{c(y_P)} \quad (18)$$

In the derivation of the formula (17) it was assumed that $p = \text{const}$, which implies the p line along the wing is straight.

Integrating by parts in Eq. (17) we obtain

$$U_\infty \alpha = \frac{p}{2\pi} \oint_{-b/2}^{b/2} \left(\frac{d\Gamma}{dy} \right)_P \frac{dy_P}{y_M - y_P} \quad (19)$$

where the integral is to be calculated according to Cauchy's principal part.

Introducing Eq. (15) in Eq. (19), the lift coefficient slope becomes

$$C_{L_\alpha} = (\pi/2p)A \quad (20)$$

Comparing Eq. (20) with Eq. (16) results, finally, in

$$p = 1 \quad (21)$$

Thus, the control point has to be chosen on the trailing edge of the wing under consideration.

According to the assumption $p = \text{const}$, the trailing edge has to be straight, which ensures that it is supersonic. The straight trailing edge result may be interpreted within the small aspect ratio wing theory⁹ as the line of maximum width beyond which, streamwise, the wing experiences no loading. However, Eq. (21) leads to errors for swept wings of very small aspect ratio ($A < 0.2$).

B. Very Large Aspect Ratio Wings with Subsonic Edges

In Ref. 11 a thorough investigation was conducted regarding the position of the control point. In the following we shall use a simplified approach by means of the formula for the calculation of the velocity induced by infinite vortex lines that intersect the inverse Mach cone of vertex M in only one point,⁴ according to Fig. 1

$$|w| = \frac{\Gamma}{2\pi d} \sqrt{M_\infty^2 \cos^2 \left(\frac{\pi}{2} - \Lambda \right) - (M_\infty^2 - 1)} \quad (22)$$

where Λ is the angle of sweep as defined in Fig. 1, and d is the distance from M to the vortex line.

For this configuration, the induced velocity takes the form

$$w(M) = \frac{\Gamma}{2\pi c} \frac{\sqrt{1 - M_\infty^2 \cos^2 \Lambda}}{\cos \Lambda} \int_0^c \frac{dx_P}{x_P - x_M} \quad (23)$$

the positive sign for w being upward.

Integrating Eq. (23) we obtain

$$w(M) = \frac{\Gamma}{2\pi c} \text{tg } \Lambda \sqrt{1 - m^2} \ln \frac{1 - p}{p} \quad (24)$$

where

$$m = \text{ctg } \Lambda \sqrt{M_\infty^2 - 1} \quad (25)$$

From the kinematic condition (14) we obtain the circulation

$$\Gamma = \frac{2\pi c U_\infty \alpha}{\text{tg } \Lambda \sqrt{1 - m^2}} \cdot \frac{1}{\ln(p/(1-p))} \quad (26)$$

Observing that in the vortex horseshoe pattern of SLLT the bound vortex is parallel to the axis Oy , the lift coefficient takes the form

$$C_L^{\text{SLLT}} = \frac{2\pi d}{\text{tg } \Lambda \sqrt{1 - m^2}} \cdot \frac{2}{\ln[p/(1-p)]} \quad (27)$$

The rigorous result derived for the two-dimensional flat plate under the supersonic small perturbations assumptions is¹³

$$C_L^{\text{theory}} = \frac{2\pi \alpha}{\text{tg } \Lambda \sqrt{1 - m^2}} \quad (28)$$

From Eqs. (27) and (28) it follows that the only point along the chord for which SLLT agrees with classical theory is given by

$$p = \frac{e^2}{e^2 + 1} \cong 0.88 \quad (29)$$

C. General Case

The two values just obtained for the position of the control point in the limiting cases of very small and very large aspect ratio wings, 100% of the chord (21) and 88% of the chord (29), are in very good agreement with the known 95% obtained by means of numerical experiments for CPM.^{2,3}

Since, as discussed earlier, for infinite wings with supersonic edges the position of the control point is arbitrary on the wing, the 88% obtained for subsonic edges ensures correct results for $A \rightarrow \infty$ regardless of the type of flow perpendicular to the edges. This leads to the idea of considering the control point position to depend on the aspect ratio. The following variation has been validated by means of comparison between the results obtained with SLLT and other reference data:

$$p = 0.88 + 0.12 \exp(-A/5) \quad (30)$$

For the usual range of aspect ratios for supersonic wing design ($A \cong 3$) the formula (30) leads to the same position of 95% of the chord mentioned earlier.

Other attempts at defining a suitable correction of the control point position for CPM panel methods are due to Lan and Mehrotra¹⁴ and Lan and Chang.¹⁵

IV. Outline of Supersonic Lifting Line Theory Application

A. Numerical Procedure

By assuming the control point position (30), the formula (10) combined with the kinematic condition (14) forms an integral equation from which the circulation Γ can be calculated. The incidence of $\alpha(y)$ in Eq. (14) should be taken as the angle between the local chord (i.e., the straight line passing through the leading and trailing edges) and axis Ox (i.e., the direction of the freestream velocity). In this way the effects of camber, washout, control surface displacement, and/or rolling motion can be accounted for in a simplified manner.

From this point on, the problem is solved similarly to the classical methods associated with theories of the lifting line type.

Thus, the total circulation will be developed in trigonometric series, similar to those used for subsonic theories

$$\Gamma(\theta) = \gamma(\theta)c(\theta) = 2bU_\infty \alpha \sum_{i=1}^N A_i \sin i\theta \quad (31)$$

where

$$y = -(b/2)\cos \theta \quad (32)$$

The main advantage of this approach is that global aerodynamic coefficients can be readily determined; for example, the lift coefficient is simply

$$C_L = \pi A_1 \alpha, \quad C_{L_\alpha} = \pi A A_1 \quad (33)$$

Moreover, a good concordance with some solutions for wings of simple planform is automatically ensured. Thus a delta wing with subsonic leading edges gives an elliptical distribution for the circulation Γ , i.e., a development into series of the form (31) with the first term A_1 dominant.^{9,13,16}

A numerical procedure, based on functional collocation, can be used to calculate the coefficients A_i (31) by means of Eq. (10).

Thus, to evaluate properly the contribution of the singularity at $y_P = y_M$, let us choose a small interval $[y_M - \epsilon', y_M + \epsilon']$, and let $w_{\epsilon'}$ be the induced velocity due to the vortices contained in this interval. By using Eq. (10) we obtain

$$-2\pi w_{\epsilon'} = \lim_{\epsilon \rightarrow 0} \left[\frac{2\Gamma(y_M)}{\epsilon} - \int_{y_M - \epsilon'}^{y_M + \epsilon'} \frac{H(x_M, y_M, y_P)}{(y_P - y_M)^2} dy_P \right] \quad (34)$$

where

$$H(x_M, y_M, y_P) = \frac{\Gamma(y_P)}{c(y_P)} [r_{LE}^H(y_P) - r_S^H(y_P)] \quad (35)$$

Over the small interval $2\epsilon'$ the variation of H can be replaced by a parabola. In this way the integrals in Eq. (34) can be calculated, the final result being

$$2\pi w_{\epsilon'} = \frac{1}{\epsilon'} [4\Gamma(y_M) - H(x_M, y_M + \epsilon', y_P) - H(x_M, y_M - \epsilon', y_P)] \quad (36)$$

The value ϵ' can be chosen in the numerical calculations so that the numerical errors are bounded by certain prescribed limits.

Outside the interval $[y_M - \epsilon', y_M + \epsilon']$ the integrals in Eq. (10) can be calculated by standard methods, for example, using Simpson's method, provided that y_P lies sufficiently far away from y_M . This restriction is generated by the fact that, to keep the truncation error of the method sufficiently small, it is necessary to decrease the integration step h when y_P approaches y_M , thus increasing the number of calculations.

It was found more economical to devise a special numerical integration method for regions adjacent to interval $[y_M - \epsilon', y_M + \epsilon']$. This method is based on approximating the numerator [the equivalent of H in Eq. (34)], instead of the whole integrand as in Simpson's method, with parabolas. Even if the special method involves more calculations (the coefficients

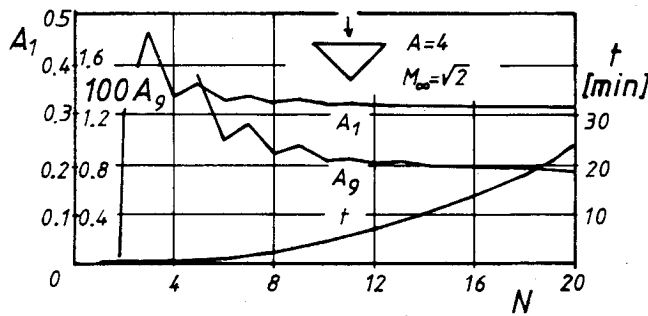


Fig. 2 Convergence test for SLLT.

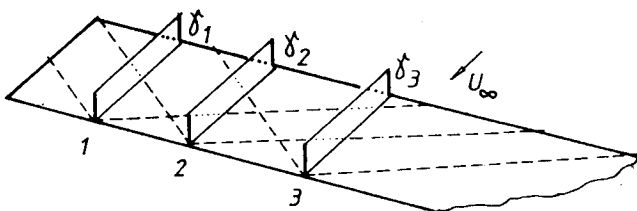


Fig. 3 Conical flows theory solutions.

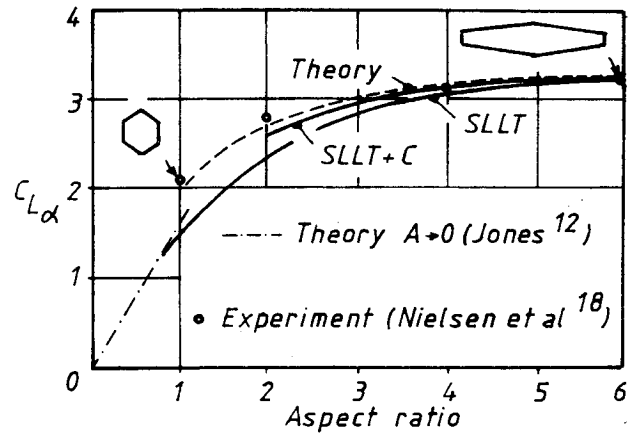


Fig. 4 Variation of lift coefficient slope with aspect ratio for straight tapered wings at $M_\infty = 1.53$.

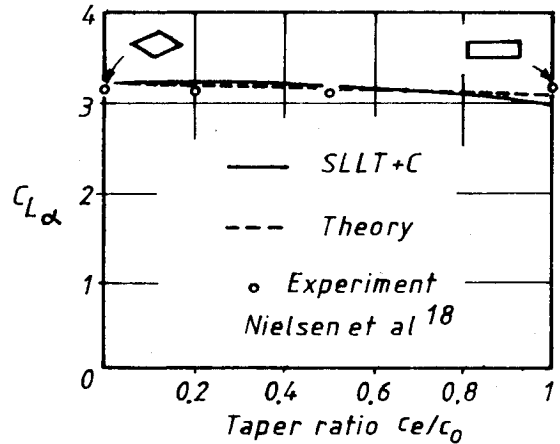


Fig. 5 Variation of lift coefficient slope with taper ratio for straight wings of aspect ratio $A = 4$ at $M_\infty = 1.53$.

used are more complex and require the evaluation of a logarithm for every second integration step), it has the advantage of depending on the much smoother variation of the numerator H (35) for y_P close to y_M .

By means of numerical experiments, a balance was achieved between the discussed method and Simpson's which led to a minimum of calculations (i.e., computer time) for a given accuracy. The resultant computer program has been written in BASIC language on an Apple IIe (8-bit microprocessor), and requires about 35 kbytes of memory.

A convergence test is presented for an inverse delta wing with sonic trailing edges (aspect ratio $A = 4$, $M_\infty = \sqrt{2}$). The variations of coefficients A_1 , A_9 , and of the execution time t vs N are shown in Fig. 2. This case was chosen as being somewhat extremal, the spanwise loading distribution being triangular. It is seen that convergence is rather good, the coefficient A_1 becoming practically constant for $N > 10$, i.e., for at least 10 terms in the development into series of circulation (31). The computing time is moderate; on the mentioned PC, the "compiled" BASIC program takes about 5 min for a development into series with 10 terms.

B. Improved Version of Supersonic Lifting Line Theory

The constant chord wing loading that enabled us to reduce the complexity of the problem induces an erroneous transfer of information between adjacent spanwise stations, as shown in Fig. 3 for a wing with supersonic edges.

For station 1 the circulation is influenced by the side edge, being somewhat smaller than the two-dimensional result. Because of the constant chord distribution, this side edge effect is transmitted spanwise to stations 2, 3, etc. This contradicts the results of linearized theory, which states that for a section such as 2, two-dimensional flow conditions should be ful-

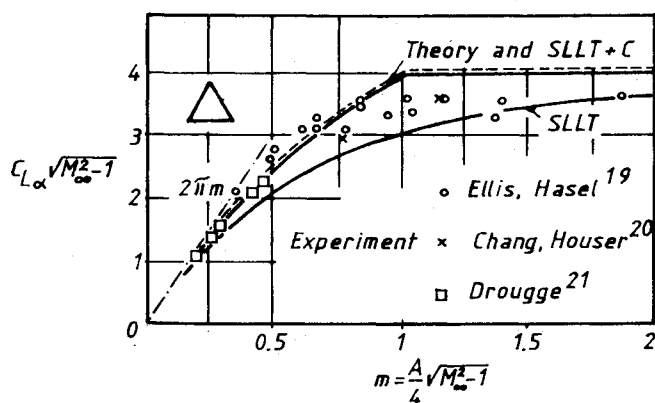


Fig. 6 Variation of lift coefficient slope with Mach number and aspect ratio for triangular wings.

filled. It follows that the SLLT approximation makes possible an information transfer beyond the inverse Mach cone limits imposed by the linearized theory. As a result of this information transfer error the circulation and, therefore, the lift coefficient are smaller than the linearized theory exact results.

To correct this kind of error, conical flow theory solutions (CFS) will be used for control points such as those denoted 2 and 3 in Fig. 3. Whereas the usual SLLT procedure leads to the calculation of the circulation by means of the integral equation approach, the modified procedure using conical flow solutions makes possible the direct calculation of the local circulation and in this way saves computing time. This improved theory has been denoted SLLT + C.

Thus, for the stations where CFS apply, the circulation is determined by closed formulas, eliminating the information transfer. Obviously SLLT + C leads to identical results to the classical theoretical ones as long as the actual flow conditions correspond to one of the conical flow solutions considered. However, the number of CFS considered in the computer program has been limited to keep the computer memory requirements to a minimum.¹⁷

V. Results

A. Isolated Wings

1. Straight Wings

The first comparison involves wings with straight 50% chord line and taper ratio $c_e/c_0 = 0.5$, of varying aspect ratio. The reference data used in Fig. 4 have been taken from Ref. 13.

Both SLLT and SLLT + C are in good agreement with the theoretical data for higher values of the aspect ratio ($A > 4$). The improved version of the supersonic lifting line theory (SLLT + C) is in better correlation with the reference data than the simple version, but its application is limited to wings of aspect ratio greater than 2.

The apparent contradiction between Jones's small aspect ratio theory,¹² which has been chosen as the target for SLLT in the limit $A \rightarrow 0$, and classical three-dimensional theoretical results might explain the differences observed in Fig. 4.

A comparison regarding the lift curve slope of straight wings with aspect ratio $A = 4$ as a function of taper ratio is presented in Fig. 5. Again, the theoretical and experimental data¹⁸ are taken from Ref. 13. The results of SLLT + C presented are in close correlation with the reference data.

The very good agreement of SLLT + C both with theoretical and experimental data for pointed wings must be noticed, whereas for untapered wings the experimental results indicate a higher lift curve slope than the classical theoretical and SLLT + C results.

2. Triangular Wings

The conical flow theory provides simple solutions for triangular wings.¹³ The improved lifting line theory (SLLT + C) will lead to similar results, since a conical flow solution corre-

sponds to any control point. Therefore, in this case we shall determine the correlation of SLLT with three-dimensional theory, and the overall agreement of theoretical results, including the lifting line approach, with the experimental data.

Some results concerning the lift curve slope of triangular wings are examined in Fig. 6, extracted from Ref. 13. The experimental data¹⁹⁻²¹ seem to confirm the classical theoretical results for small leading-edge parameters $m < 1$, i.e., for the case: the flow normal to the leading edge is subsonic [see the formula (25)]. However, the same is not true for larger values of m . Examining the results it can be seen that for $m > 1$ the simple lifting line theory yields better correlated results with the experiment than the more accurate theoretical ones. As discussed in Ref. 4 this is probably due to some canceling between the errors involved in the SLLT model.

It can be observed from Fig. 6 that the two lifting line versions, SLLT and SLLT + C, encompass the experimental data. These differences conveniently point out the precision of the supersonic lifting line theory, which is broadly similar to other theories based on the small disturbance assumptions.

The same identity between SLLT + C and exact linearized results can be inferred from Fig. 7, which deals with the spanwise loading over triangular wings. It can also be observed that the spanwise load distribution yielded by the two versions of SLLT is in much better agreement than the global results.

3. Swept Wings

The swept wings are probably the most difficult to be treated under the supersonic lifting line assumption. This is due to the large differences between the constant chord loading approximation (2) and the exact theoretical one.

In Fig. 8 is presented a comparison for untapered wings with subsonic edges and different sweep parameters $m = \text{ctg } \Lambda \sqrt{M_\infty^2 - 1}$ where Λ is the sweep angle. The reference theoretical curves are based on the theories of Cohen²² and Mirels²³ and have been extracted from Ref. 13. It can be observed that

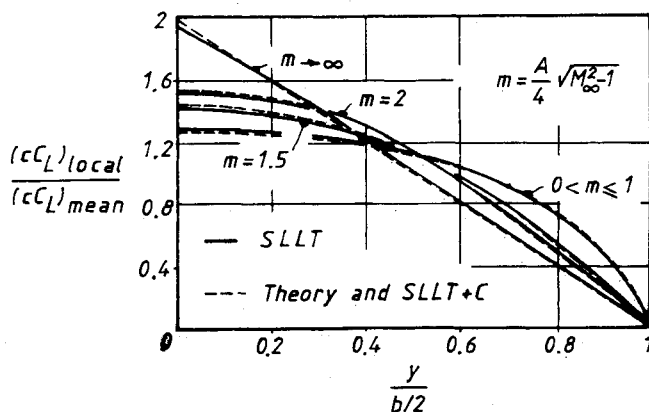


Fig. 7 Spanwise load distribution on triangular wings.

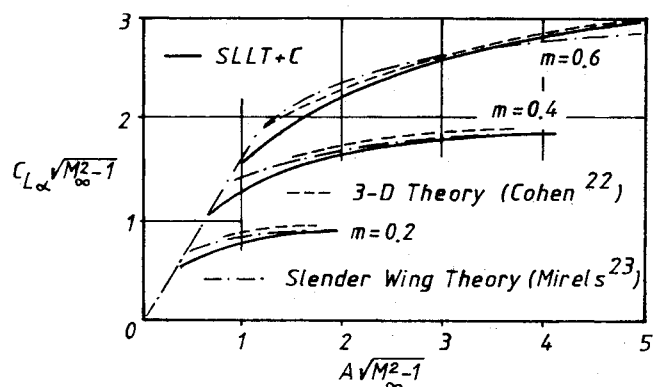


Fig. 8 Variation of lift coefficient slope with reduced aspect ratio for untapered wings with supersonic edges.

the results of SLLT + C are in good agreement with the theoretical data considered.

The results of SLLT are not plotted since they are rather imprecise.¹¹ The reason was already outlined for straight wings, when the apparent contradiction between Jones's theory¹² and three-dimensional theoretical results have been pointed out.

In Fig. 9 a few examples are given of lift curve slope variation as a function of Mach number, aspect ratio, leading edge sweep Λ and taper ratio. The theoretical results presented here have been extracted from Ref. 24 and refer to the specific case of subsonic leading edge and supersonic trailing edge, while the tip Mach cones do not intersect on the wing. These conditions limit the applicability of the reference theory (see Fig. 9). The results of SLLT + C are in good agreement with the theoretical data considered.

The variation of the damping in roll derivative C_{lp} is presented in Fig. 10 similarly to Fig. 9. The comparison is based on the same theoretical results.²⁴

For the case of the rolling wing it is not possible to use the SLLT + C approximation because only flat plate ($\alpha = \text{const}$)

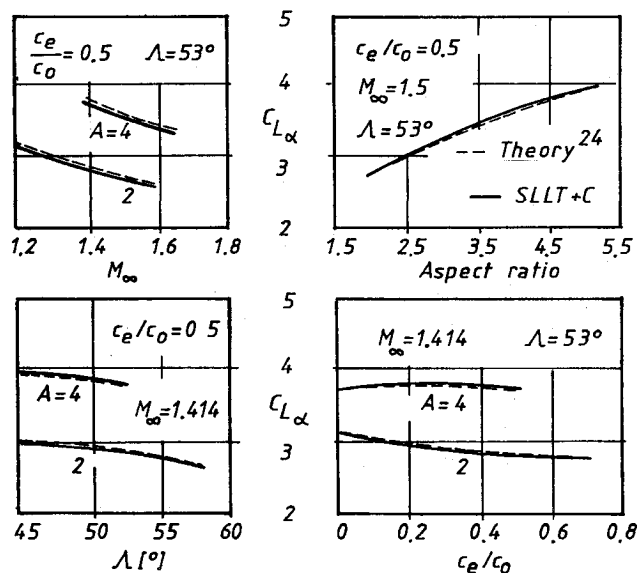


Fig. 9 Variation of lift coefficient slope with Mach number, aspect ratio, leading-edge sweep, and taper ratio.

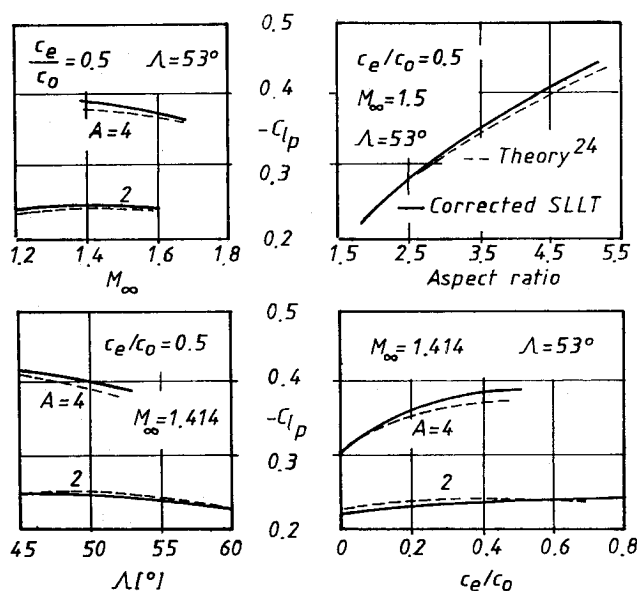


Fig. 10 Variation of damping in roll derivative with Mach number, aspect ratio, leading-edge sweep, and taper ratio.

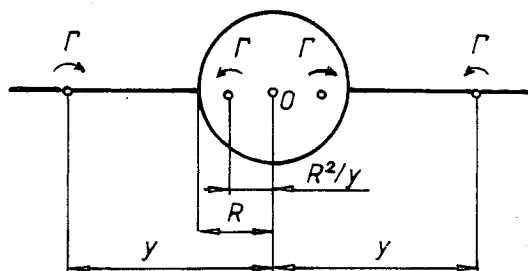


Fig. 11 Free vortex line "image."

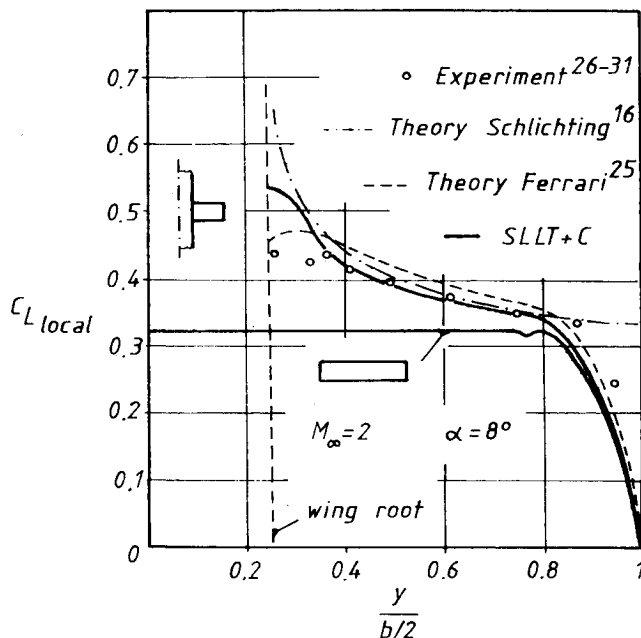


Fig. 12 Spanwise load distribution for a rectangular wing with $A_{\text{eff}} = 4.29$ in the presence of a circular fuselage.

conical flow solutions have been considered in the SLLT + C program.

The "corrected" lifting line results presented here have been obtained by multiplying the result of SLLT with a global correction factor obtained as the ratio of the lift curve slopes that resulted in the approximations of SLLT + C and SLLT, respectively. Thus, it is considered that the spanwise distribution yielded by SLLT is correct (this assumption is supported by the comparisons regarding spanwise load distributions for triangular wings in symmetrical evolutions), and a correction is done by means of the mentioned global factor. From Fig. 10 it may be observed that the corrected SLLT results are in good correlation with the theoretical results.²⁴

B. Wing-Body Combinations

The velocity induced by an infinite vortex line parallel to the Ox axis under the supersonic linearized flow assumption is⁴

$$|\vec{V}(M)| = \Gamma / 2\pi d \quad (37)$$

Since this result is identical to the one for incompressible flows, the same modeling of the interference between wing and body will be used. Thus, the fuselage will be considered an infinite circular cylinder parallel to Ox . From the condition that the flow is tangent to the fuselage it follows that each free vortex line on the wing has an "image," located according to Fig. 11. A vortex line located in the center of the circular cylinder appears only for asymmetrical load distributions.

The second effect accounted for regards the modification of the angle of attack on the wing due to the presence of the fuselage. The small perturbations assumption leads to the conclusion that the crossflow on the fuselage may be described by means of the incompressible flow relations. For an infinite

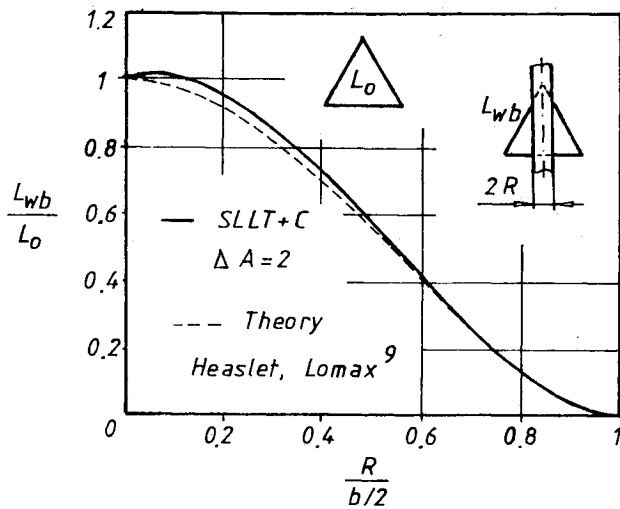


Fig. 13 Ratio of the lift of the wing body combination and isolated wing as a function of fuselage radius.

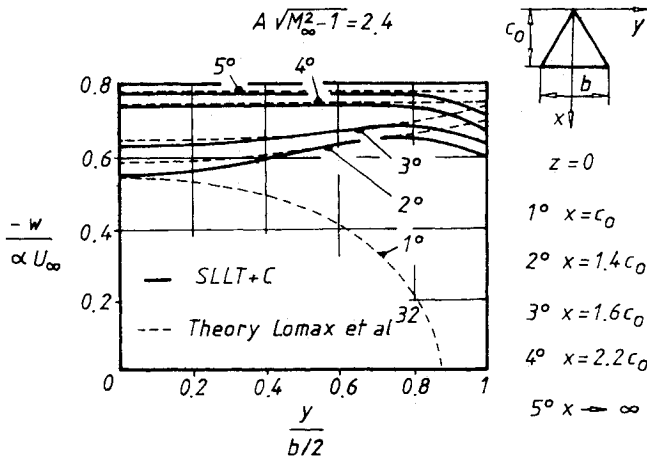


Fig. 14 Spanwise downwash distributions for triangular wings.

circular cylinder, the two-dimensional theory shows that for $y_M > R$ the modification of the angle of attack is given by^{16,25}

$$\frac{\Delta\alpha}{\alpha} = \frac{R^2}{y_M^2} \quad (38)$$

where the wing was assumed to be midpositioned on the fuselage, according to Fig. 11. The numerical procedure is similar to the one just described. Because of the singularity situated at the wing root ($|y_M| = R$) this spanwise station is avoided.

In Fig. 12 the spanwise load distribution on a rectangular wing installed at zero incidence on a circular body with ogival nose is plotted. The experimental results have been obtained at Cornell Aeronautical Laboratory²⁶⁻³¹ and were extracted from Ref. 25. The reference theoretical curves have been calculated according to Refs. 16 and 25. The same distribution for the isolated wing is presented for the sake of comparison.

The simplified theory devised by Schlichting¹⁶ takes into account only the modification of the local incidence (38) produced by the fuselage. The wing calculation assumes each spanwise station to act as a two-dimensional profile, while the incidence is variable.

Since in the present method this effect is considered in a similar way, the results agree in that region of the wing where the characteristics are quasibidimensional. Of course, the agreement is less good at the root and tip where the flow is no longer bidimensional.

The comparison of the results obtained with the SLLT method also shows good correspondence with the method of Ferrari²⁵ and with the experimental data.²⁶⁻³¹

The global coefficients are also well approximated. Thus, the total lift on the wing (based on the effective wing area) is $C_L = 0.362$ for SLLT as compared to $C_L = 0.3625$ in the experiments and $C_L = 0.3734$ for Ferrari's method. The spanwise load distribution for the wing alone is also presented in Fig. 12 to emphasize the effect of the fuselage.

The comparison in Fig. 13 is of the ratio of the wing-body combination lift to the reference triangular wing ($R = 0$) lift, as a function of fuselage radius to semispan ratio. The reference data are based on the slender body theory presented in Ref. 9. The configuration consists of a delta wing midpositioned on an infinite circular fuselage. The wing incidence on the fuselage is $\alpha = 0$. It can be observed that the results of SLLT are in good agreement with the reference theory.

C. Wing-Tail Combinations

The application of SLLT to the calculation of wing-tail interference is quite straightforward, involving the following steps¹⁰: 1) the calculation of the aerodynamic loading on the first (isolated) wing, by means of SLLT + C, 2) the calculation of the upwash; and 3) the calculation of the second wing aerodynamic loading with the wake influence of the first one. The following comparisons concern especially the second step, since the first and third ones are standard wing calculations and as such have already been assessed for isolated wings.

The downwash behind a delta wing with the sweep parameter $A\sqrt{M_\infty^2 - 1} = 2.4$ is presented in Fig. 14. The reference data have been calculated by Lomax et al.³² within the linearized theory assumptions without further approximations.

It must be observed that for $x = c_0$ the results of SLLT + C have not been plotted because of the inherent error due to the proximity of the control point (where the downwash equals unity). The downwash calculated with the supersonic lifting line theory is in good agreement with the exact linearized one. The only departure takes place toward the tip, where SLLT + C indicates a small drop of the downwash.

It has been shown^{6,32} that the upwash tends to infinity when the point M is situated on the Mach cone issuing from the tip. The same result is also true for the case of SLLT.¹⁰

In Fig. 15 data are presented concerning the downwash behind a rectangular wing of aspect ratio $A = 3.5$ at $M_\infty = 1.53$. The reference theoretical and experimental³³ data have been extracted from Ref. 34. Although the agreement of the SLLT + C results with the experimental results is not as good as that of the reference theory, the supersonic lifting line theory provides a useful estimate.

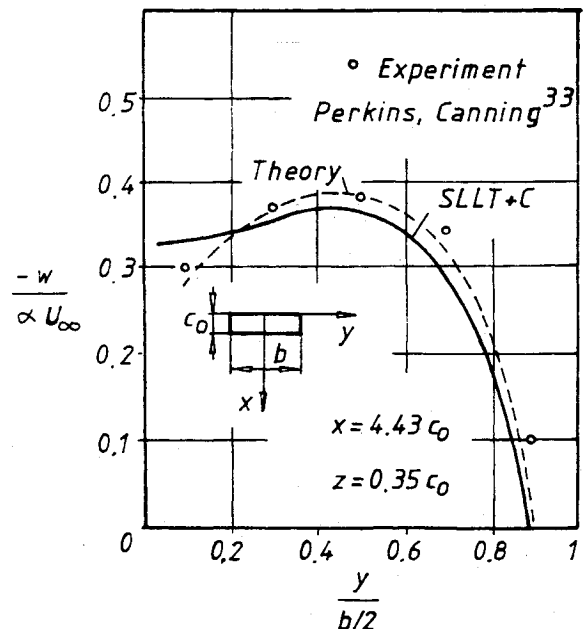


Fig. 15 Downwash behind a rectangular wing with $A = 3.5$ at $M_\infty = 1.53$.

It should be mentioned that the experimental results presented refer to small incidence, $\alpha \approx 0$. The theoretical linearized results fail to account for nonlinear effects which become more important for higher angles of attack.

VI. Conclusions

The supersonic lifting line theory (SLLT) surveyed in this paper enabled us to obtain some interesting results regarding the control point position, which seem to be useful for the related constant pressure panel (CPM) methods.^{2,3} Thus, it is found that the chordwise position of the control point must be 100%*c* for small aspect ratio wings and 88%*c* for very large aspect ratio wings with subsonic edges. These limits are in very good agreement with the known 95%*c* obtained by means of numerical experiments for CPM. A formula is proposed for the correlation of the control point position with the aspect ratio which might prove to be useful for CPM as well.

Accuracy of SLLT is shown to be completely compatible with the small perturbations assumptions under which it was derived. The comparisons regarding the aerodynamic calculation of isolated wings,³⁵ wing-body,³⁶ and wing-tail¹⁰ configurations showed good correlation with a wide range of reference theoretical and experimental data.

References

- ¹Prandtl, L., *Tragflügeltheorie*, I. and II. Mitteilung, Nachrichten der Königl. Gesellschaft für Wissenschaften, Göttingen, Math.-Phys. Klasse 1918, pp. 451-477, and 1919, pp. 105-137.
- ²Woodward, F. A., "Analysis and Design of Wing-Body Combinations at Subsonic and Supersonic Speeds," *Journal of Aircraft*, Vol. 5, No. 6, 1968, pp. 528-534.
- ³Woodward, F. A., "An Improved Method for the Aerodynamic Analysis of Wing-Body-Tail Configurations in Subsonic and Supersonic Flow. Part I: Theory and Applications; Part II: Computer Program Description," NASA CR-2228, May 1973.
- ⁴Constantinescu, V. N., and Jadic, I., "On a Lifting Line Theory for Supersonic Flow. I) The Velocity Field due to a Vortex Line in Supersonic Flow," *Revue Roumaine des Sciences Techniques Serie de Mecanique Appliquee*, Vol. 34, No. 5, 1989, pp. 439-452; "II) A Supersonic Lifting line Theory for Wings," *Revue Roumaine des Sciences Techniques Serie de Mecanique Appliquee*, Vol. 34, No. 6, 1989, pp. 553-565.
- ⁵Ackert, J., "Luftkräfte auf Flügel, die mit grösserer als Schallgeschwindigkeit bewegt werden," *Zeitschrift für Flugtechnik und Motorluftschiffahrt*, 1925, pp. 72-74; also, English translation NACA TM 317, 1925.
- ⁶Mirels, H., and Haefeli, R. C., "Line Vortex Theory for Calculation of Supersonic Downwash," NACA Rept. 983, 1950.
- ⁷Laschka, B., "Untersuchungen über das Abwindfeld hinter Tragflügeln bei Überschallgeschwindigkeit," *Zeitschrift für Flugwissenschaft*, 1960.
- ⁸Jadic, I., "Calculation of the Velocity Field Induced by a Vortex Distribution in Supersonic Regime," *Revue Roumaine de Mathematiques Pures et Appliquees*, Vol. 34, No. 6, 1989, pp. 545-551.
- ⁹Heaslet, M. A., and Lomax, H., "General Theory of High Speed Aerodynamics, Sec. D: Supersonic and Transonic Small Perturbation Theory," Vol. VI, *High Speed Aerodynamics and Jet Propulsion*, edited by W. R. Sears, Princeton Univ. Press, Princeton, NJ, 1954.
- ¹⁰Jadic, I., "Aerodynamic Calculation of Tandem Wings in Supersonic Flow by Means of SLLT," *Revue Roumaine des Sciences Techniques Serie de Mecanique Appliquee*, Vol. 35, No. 4, 1990, pp. 309-324.
- ¹¹Jadic, I., "A Verification of the Supersonic Lifting Line Theory for the Case of Infinite Yawed Wings," *Revue Roumaine des Sciences Techniques Serie de Mecanique Appliquee*, Vol. 35, No. 1, 1990, pp. 17-32.
- ¹²Jones, R. T., "Properties of Low Aspect Ratio Pointed Wings at Speeds below and above the Speed of Sound," NACA Rept. 835, 1946.
- ¹³Jones, R. T., and Cohen, D., "Aerodynamic Components of Aircraft at High Speeds, Sec. A: Aerodynamics of Wings at High Speeds," Vol. VII, *High Speed Aerodynamics and Jet Propulsion*, edited by A. F. Donovan and H. R. Lawrence, Princeton Univ. Press, Princeton, NJ, 1957.
- ¹⁴Lan, C. E., and Mehrara, S. C., "An Improved Woodward's Panel Method for Calculating Leading-Edge and Side-Edge Suction Forces at Subsonic and Supersonic Speeds," NASA CR-3205, Nov. 1979.
- ¹⁵Lan, C. E., and Chang, J. F., "Calculation of Vortex Lift Effect for Cambered Wings by the Suction Analogy," NASA CR-3449, July 1981.
- ¹⁶Schlichting, H., and Truckenbrodt, E., *Aerodynamik des Flugzeuges*, Springer, 1960.
- ¹⁷Jadic, I., "On the Improvement of the Supersonic Lifting Line Theory," *Revue Roumaine des Sciences Techniques Serie de Mecanique Appliquee*, Vol. 35, No. 2, 1990, pp. 75-88.
- ¹⁸Nielsen, J. N., Matteson, F. H., and Vincenti, W. G., "Investigation of Wing Characteristics at a Mach Number of 1.53; III: Unswept Wings of Differing Aspect Ratio and Taper Ratio," NACA RM A8E06, 1948.
- ¹⁹Ellis, M. C., Jr., and Hasel, L. E., "Preliminary Tests at Supersonic Speeds of Triangular and Sweptback Wings," NACA RM 26L17, 1947.
- ²⁰Chang, C. C., and Houser, J. E., "Correlation of Test Data and Comparison with Theoretical Results for Thin Wings in Supersonic Flow," Glenn L. Martin Co. Engineering Rept. 2729, 1947.
- ²¹Drougge, G., "Some Measurements at Low Supersonic Speeds by a Method for Continuous Variation of the Mach Number," FFA Rept. 42, 1952.
- ²²Cohen, D., "Formulas for the Supersonic Loading, Lift and Drag of Flat Sweptback Wings with Leading Edges behind the Mach Lines," NACA Rept. 1050, 1951.
- ²³Mirels, H., "Aerodynamics of Slender Wings and Wing-Body Combinations Having Swept Trailing Edges," NACA TN 3105, 1954.
- ²⁴Malvestuto, F. S., Jr., Margolis, K., and Ribner, H. S., "Theoretical Lift and Damping in Roll at Supersonic Speeds of Thin Sweptback Tapered Wings with Streamwise Tips, Subsonic Leading Edges, and Supersonic Trailing Edges," NACA Rept. 970, 1950.
- ²⁵Ferrari, C., "Aerodynamic Components of Aircraft at High Speeds, Sec. C: Interaction Problems," Vol. VII, *High Speed Aerodynamics and Jet Propulsion*, edited by A. F. Donovan, and H. R. Lawrence, Princeton Univ. Press, Princeton, NJ, 1957.
- ²⁶Cramer, R. H., "Interference between Wing and Body at Supersonic Speeds, Pt. V: Phase One Wind Tunnel Tests Correlated with the Linear Theory," Cornell Aeronautical Lab., Bumblebee Rept. CAL/CM-597, Dec. 1950.
- ²⁷Dye, F. E., Jr., "A Comparison of Pressure Predicted by Exact and Approximate Theories with Some Experimental Results on an Ogival-Nosed Body at a Mach Number of 2.0," Cornell Aeronautical Lab., Bumblebee Rept. CAL/CF-1723, Dec. 1951.
- ²⁸Berler, I., and Nichols, S., "Interference between Wing and Body at Supersonic Speeds, Part. VI: Data Report on Pressure Distribution Tests of Wing-Body Interference Models at Mach Number 2.0," Phase Two Tests of June 1949, Cornell Aeronautical Lab., Bumblebee Rept. CAL/CF-1569, May 1951.
- ²⁹Berler, I., and Nichols, S., "Interference between Wing and Body at Supersonic Speeds, Pt. VII: Data Report on Pressure Distribution Tests of Wing-Body Interference Models at Mach Number 2.0," Phase Three Tests of August 1949, Cornell Aeronautical Lab., Bumblebee Rept. CAL/CF-1570, June 1951.
- ³⁰Nichols, S., "Interference Between Wing and Body at Supersonic Speeds, Pt. VIII: Data Report on Pressure Distribution Tests of Wing-Body Interference Models at Mach Number 2.0," Phase Four Tests of March 1950, Cornell Aeronautical Lab., Bumblebee Rept. CAL/CF-1571, July 1951.
- ³¹Dye, F. E., Jr., "Interference Between Wing and Body at Supersonic Speeds, Pt. IX: Data Report on Pressure Distribution Tests of Wing-Body Interference Models at Mach Number 2.0," Phase Five Tests of August 1951, Cornell Aeronautical Lab., Bumblebee Rept. CAL/CF-1684, Dec. 1951.
- ³²Lomax, H., Sluder, L., and Heaslet, M. A., "The Calculation of Downwash behind Supersonic Wings with an Application to Triangular Planforms," NACA Rept. 957, 1950.
- ³³Perkins, E. W., and Canning, T. N., "Investigation of Downwash and Wake Characteristics at a Mach Number of 1.53. P. I: Rectangular Wing," NACA RM A8L16, 1949.
- ³⁴Frick, C. W., "Aerodynamic Components of Aircraft at High Speeds, Sec. G: The Experimental Aerodynamics of Wings at Transonic and Supersonic Speeds," Vol. VII, *High Speed Aerodynamics and Jet Propulsion*, edited by A. F. Donovan, and H. R. Lawrence, Princeton Univ. Press, Princeton, NJ, 1957.
- ³⁵Jadic, I., "Wing Calculation in Supersonic Flow by Means of the Supersonic Lifting Line Theory," *Revue Roumaine des Sciences Techniques Serie de Mecanique Appliquee*, Vol. 35, No. 3, 1990, pp. 197-208.
- ³⁶Jadic, I., "The Calculation of Wing-Body Interference in Supersonic Flow by Means of SLLT," *Zeitschrift für angewandte Mathematik und Mechanik* (to be published).